METAL OXIDE BASED NANOSTRUCTURE ENGINEERING: ELECTRICAL AND GAS SENSITIVE PROPERTIES OF STRUCTURALLY MODIFIED SnO_2 NANOWIRES

S. Dmitriev

Physics Department, Moldova State University, 60, A. Mateevici str., MD-2009, Chisinau, Republic of Moldova
E-mail: sdmitriev@usm.md
(Received 3 July 2009)

Abstract

The paper presents results of the research aimed at the engineering of nanostructures (NSs). SnO_2 nanowires (NWs) were grown via vapor-solid mechanism at a synthesis temperature of 900°C in a modified set-up allowing the NS morphology be encoded in a programmable way along its length. The Ti/Au (20/500 nm) electrical contacts to individual NWs were deposited via consequent PVD vacuum deposition process to obtain gas sensitive chemiresistors.

Electrical properties and gas-sensing performance of the obtained monocrystalline NSs with a modified shape were investigated using hydrogen and oxygen gases. It was established that structurally modified NWs, due to the presence of narrow segments, exhibit better gas-sensitive characteristics in comparison with straight NWs. Obtained results are discussed from the positions of single-crystal "neck" formation in NSs and their influence on transport properties of NWs.

1. Introduction

A series of recent publications has demonstrated that one-dimensional (1D) nanostructures (NSs) on the basis of metaloxides possess a huge potential for application in the quality of chemical and biological sensors [1-10]. The latter is related to their generic chemical and thermal stability, their innate ability to transduce surface events into electrical signals and to the following two very important features of 1D NSs: (1) very high surface-to-bulk (*S/B*) ratio; (2) comparability of the Debye screening length L_D with the effective radius R of the conducting channel in NWs. Both these factors play a determining role in the sensing performance of NSs. In particular, the larger the *S/B* and L_D /*R* ratios of the active gas sensitive element the higher its sensitivity.

The performance of chemoresistor gas sensors (GSs) and especially their sensitivity are determined by their material-specific surface chemistry as well as the size and shape of their active elements. Currently, three basic approaches are used in nanomaterials based GS developments. The first one is based on the fabrication of very fine nanoparticle agglomerates [11]; the second approach is connected with preparation of the metaloxide polycrystalline nanodimensional and nanostructured films [12-14]; and the third one relies on single crystal NSs (NWs, nanorods, nanoribbons etc.) as sensing elements [1-6]. Both high *S/B* and L_D /*D* ratios can be achieved using all three mentioned approaches. However, the first two approaches face the traditional challenges resultant from the unstable nature of the inter-granular interface, which determines the connectivity between grains [15] and hence the reliability, reproducibility, and "lifetime" of the performance of the device. Thermomechanical and thermochemical instabilities of contacts are potentially other shortcomings of particle-aggregate-based gas sensors operating (as is often the case) at high temperatures and reactive environment.

The major advantage of single crystal quasi-1D sensors over traditional granular material based sensors is their conducting channel well-defined structurally and compositionally, which does not rely on intergrain junctions for conductance. Thus, sensors based on single crystal metaloxide 1D NSs allow, in principle, drastic improving of the majority of the aforementioned limitations. However, to compete with the operation parameters of the best available polycrystalline film sensors the nanowires, as sensitive elements of GS, should possess an effective diameter in the order of 10-20 nm. Only in this case, we can obtain the ratio $L_d/R \sim 1$ (where L_d is the Debye screening length and R is the effective size (radius) of NW), i.e., the condition when NW sensitivity or responsiveness reaches the maximum due to the complete depletion of the NW. However, such NSs belong to the size range where it is still challenging to produce NSs in a controllable way to fabricate reliable electronic devices.

To overcome these technical challenges and to use the advantages of NW's crystallinity in full degree, the utilization of the quasi-1D metal oxide NSs with modified morphology in the quality of gas sensitive elements (GSEs) may be considered. Each such GSE can consist of a series of few micron long mesoscopic (300-400 nm in diameter) segments connected via ultra short and thin (tens of nanometers in length and diameter) ones. The physics behind this approach is illustrated schematically in Figure 1. For simplicity, only one section of the developed NW, consisting of two long segments and a short one between them, is presented in Fig. 1 for illustration.

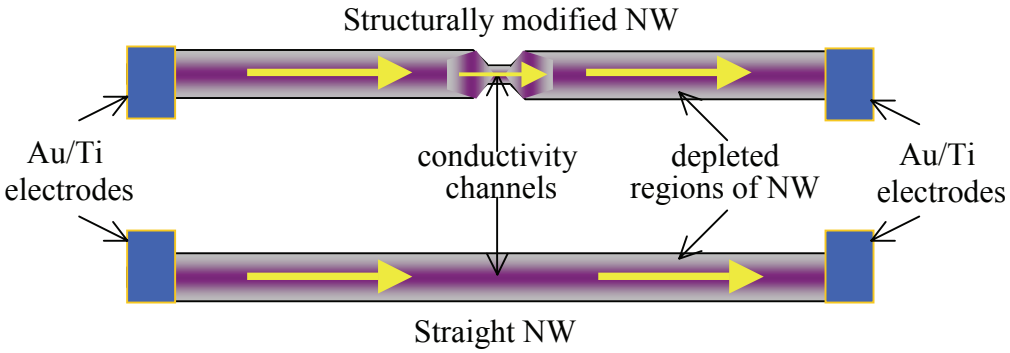

Fig. 1. Structures of and electrical current in structurally modified and straight metal oxide NW based GSEs.

Here we have the NS with periodically alternating cross-section. It is important to note that, in our case, in the contrast to granular structures, where the "necks" are formed by the contacts of neighboring grains and electrical current is modified by Schottky barriers, the "neck" region is a part of the same single crystal NW and the electrical transport through such NS will be determined by the adsorbate-induced alternation in the effective cross-section of the conductivity channel. For comparison of the modes of electrical current passing, the straight NW based GSE is also shown. Taking into account that physical/geometrical diameter of the "neck" region of the NW is at least one order less than the diameter of the basic part of the NW, we can expect that the sensitivity of this narrowed region to adsorption-desorption processes will be higher.

Thus, this experimental work was aimed to verify the applicability of the proposed approach to improve the gas sensing performance of the GSE via its structural modulation.

2. Experimental

SnO_2 single-crystal structurally modified and also straight NWs were fabricated via traditional vapor-solid growth process [16] in a Lindberg/Blue Scientific tube furnace at the

temperature T=900°C from the powder precursor. However, some modifications to the process on the basis of recently developed techniques [17, 18], which allow programming the morphology of metal oxide NSs during their synthesis, were used. Briefly, argon (99.998%), used as a carrier gas, was fed into a quartz tube through a solenoid valve activated by a computer-controlled power supply, allowing the argon gas flow to be shut off and turned on in a programmable sequence.

X-ray diffraction (XRD) and Scanning Electron Microscopy were used to characterize the structure, composition, and shape of the SnO_2 NWs.

Resist-free, Ti/Au (20/500 nm) PVD vacuum deposition through a shadow mask was used to produce ohmic electrical contacts to individual segmented NWs and fabricate NW based chemical sensor.

The electrical (I-V) and gas sensing properties of the SnO_2 NWs were measured in the range -5 to +5 Volts in the two-probe mode at the different temperatures of the 100-350°C range under vacuum conditions $P=1x10^{-6}$ Torr and with sequential oxygen and hydrogen exposures in the range from $1x10^{-5}$ to $6x10^{-4}$ Torr. Gas pressure in the chamber was maintained by means of the pneumatic needle valves programmed by the *LabView* computer program.

3. Results and discussion

3.1. Structural characterization of SnO_2 NWs

Figure 2 demonstrates XRD spectra of as-grown SnO_2 NWs (both straight and structurally modified) obtained in the 25-60° 2θ range. One can see that reflection peaks are very narrow, which confirms that the grown NWs are highly crystalline. Observed peaks are characteristic of tetragonal (rutile) SnO_2 with domination of the signal reflected from (101) crystallographic plane. Other peaks obtained from (110) and (200) planes are twice less in magnitude. As to the peaks assigned to (111), (210), (211), and (220) planes, they are not pronounced.

SEM image of the tin dioxide single-crystal structurally modified NW (SMNW) confined between two Au/Ti electrodes (Fig. 3) shows that it consists of alteration of the well-faceted segments of different diameter. From TEM images (not presented here), it was estimated that effective diameters of changing segments are in the range from ~ 40 to about 290 nm. Lengths of both types of NWs amounted to 12-15 μm.

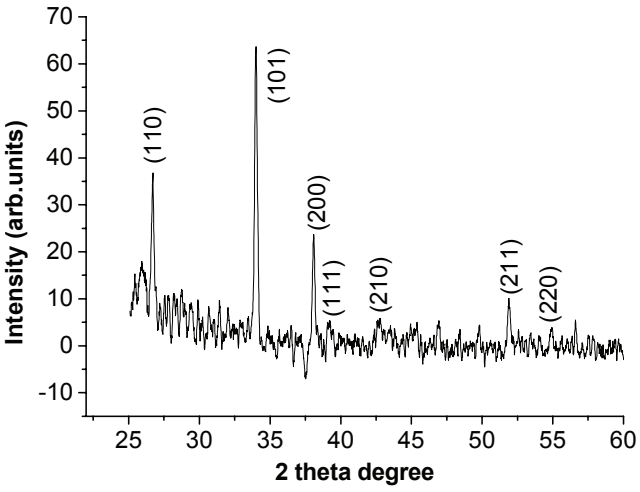

Fig. 2. XRD spectrum of SnO_2 NWs.

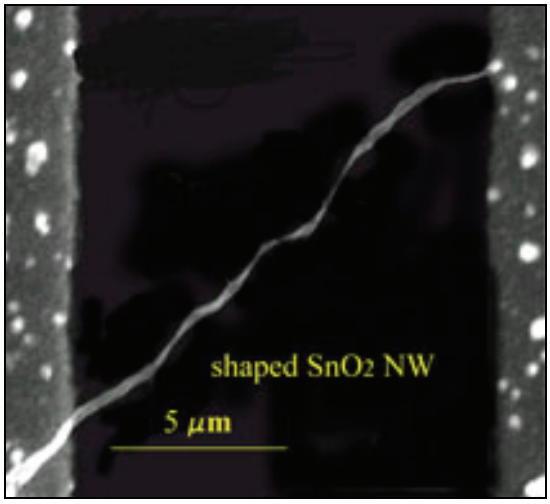

Fig. 3. SEM image of SnO_2 SMNW with two Au/Ti electrodes.

3.2. Electrical and gas sensing characterization of SnO_2 NWs

The I-V curves of the tin dioxide SMNW were measured in the temperature interval from 100 to 350°C (working diapason of gas sensors) in vacuum and in the presence of oxygen (P_{O2}=1x10^{-4} Torr), because oxygen plays an exclusively important role in the gas detection processes, determining, in general, the sensing performance of the device. It was found that the measured I-V curves are linear with applied voltage throughout the entire temperature range, implying ohmic contacts both under vacuum and in the presence of oxygen—an important factor if these NSs are to be used as sensors. Figure 4 shows one representative I-V dependence graph for T_{meas}=250°C. However, one can see an asymmetric behavior of curves. In particular, current magnitudes at ± 5 V are in some degree different for both vacuum and oxygen cases. In our opinion, this may be due to different resistances between NWs and electrodes themselves, i.e., different lengths of NW ends are covered with electrodes and, as a result, different contact areas between NW and electrode for each NW end.

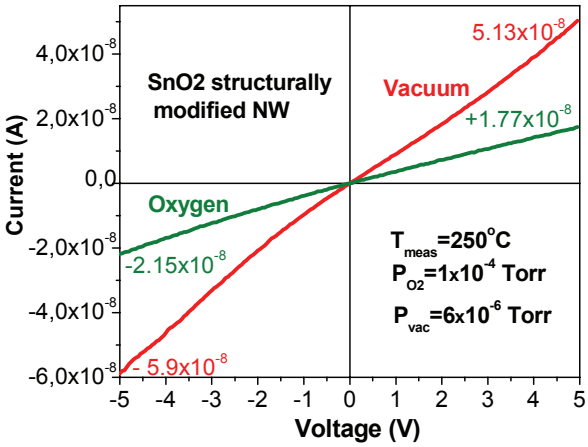

Fig. 4. Typical I(V) dependences of tin dioxide SMNW in vacuum and in the presence of oxygen.

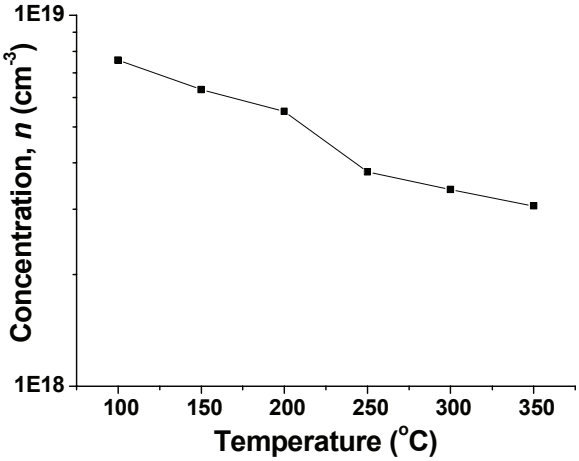

Fig. 5. Dependence n=f(T) for tin dioxide SMNW in the presence of O_2.

It is interesting to estimate the ratio of the currents through an NW in the presence of O_2 and under vacuum conditions, i.e., sensitivity to oxygen itself. In our case, the value of I_{oxy}/I_{vac} ratio to 1x10^{-4} Torr oxygen is ~2.8 that can provide the equivalent of sensitivity toward 100 ppb of O_2 dissolved in the inert gas being at atmospheric pressure. One can see that tin dioxide NWs are very sensitive to oxygen and can actively adsorb it. Also, we observe the linear growth of S_{oxy}= I_{oxy}/I_{vac} on the dependence on applied voltage. However, large biases can lead to the NW destroying due to electrical breakdown, so we restricted ourselves to ± 5 V range.

Figure 5 shows the calculated dependence of electron concentration *(n)* on temperature derived from the I-V data obtained at temperatures from 100 to 350°C in the oxygen presence. First of all, we should note that the values of *n* estimated from I-V data are reasonable, i.e., are in the range 10^{18}-10^{20} cm^{-3} characteristic of SnO_2 materials. Secondly, when plotted at *n*=f(T), two linear regions (100-200°C and 250-350°C) and a transition region (200-250°C) are observed for this function, which can be assigned to the peculiarities of the adsorption/desorption processes occurring at the SnO_2 NW surface. Namely, as it was shown for SnO_2 films, below 180°C, oxygen is adsorbed as a molecular species O_2^- [12]. From this temperature and up to ~250°C, the molecular oxygen undergoes the surface dissociation reaction $O_2 + e^- \rightarrow 2O^-$. The latter, in an ideal case, should lead to the doubling of the reactive oxygen species adsorbed on

the surface and, as result, the twofold decrease in the free carrier concentration in the NW. In reality, the situation is quite different, as one can see from Fig. 5. In particular, the n_{150}/n_{300} ratio of the free electron concentrations at 150 and 300°C, respectively (taken from two linear regions), is 1.93. This difference from 2 can be stipulated by very different factors. In particular, the following factors can be considered as reasons for the observed discrepancy: (1) probability of adsorption of O^- radicals depends on the amount of the free surface sites available for adsorption; (2) inertia of adsorption–desorption processes; (3) state of the surface (cleanness). Nevertheless, we can state that this feature, which is characteristic of thin film sensors, is kept also at the nanoscale. The value of the conductance activation energy estimated from the log n=f(T) dependence was in a range of ~80-100 meV that corresponds to the energy range of the oxygen vacancy donor levels below the conduction band edge in SnO_2 [19].

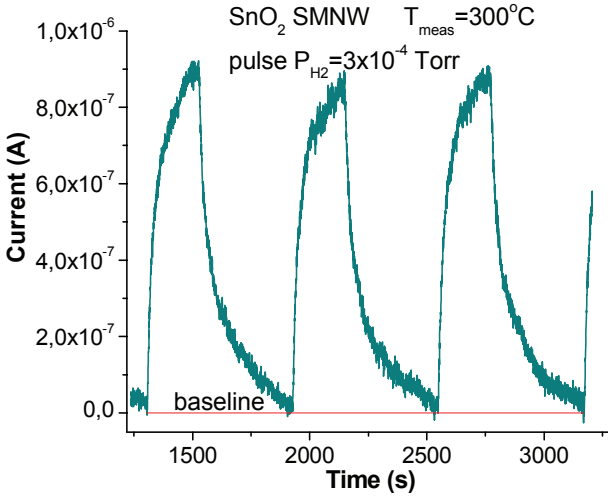

Fig. 6. Current response of SnO_2 SMNW to hydrogen gas pulses.

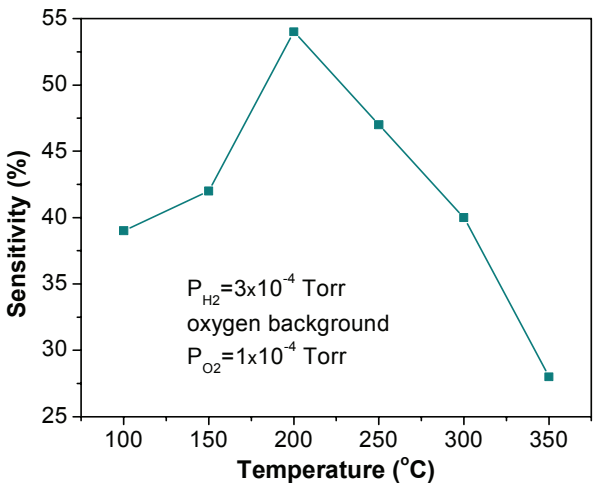

Fig. 7. Temperature dependence of SMNW gas sensitivity to H_2.

Figure 6 demonstrates the typical SMNW response toward $3x10^{-4}$ Torr hydrogen pulses at the measurement temperature T=300°C. The magnitude of oxygen background was kept on the level $P_{O2}=1x10^{-4}$ Torr to provide required level of SMNW sensibilization. Baseline corresponds to the current through NW under vacuum conditions. One can see that H_2 leaking-in into the test chamber leads to the increase of conductivity through SMNW that corresponds to behavior of *n*-type material in the reducing atmosphere. As in traditional thin film or ceramic based SnO_2 sensors, the interaction of hydrogen with oxygen and hydroxyl groups chemisorbed on the NW surface leads to the formation of water molecules, which at these temperatures are desorbed from NW surface. This process is accompanied by electron release back to the conduction band of metal oxide NW and, as a result, determines the consequent NW resistance decrease and current growth.

Results of the measurements of SMNW gas sensitivity to H_2 (determined as $S=\Delta I/I_0 \cdot 100\%$) as a function of the operation temperature are presented in Fig. 7. One can see that the temperature maximum of sensitivity to hydrogen takes place at the temperature $T_{max}=200$°C and amounts to 54%. Recalculation of hydrogen partial pressure from Torr to ppm gives the hydrogen concentration on the level of 0.39 ppm (oxygen background is 0.13 ppm). The observed on S=f(T) maximum is related to the competition of at least two surface processes: the thermally activated reaction with pre-adsorbed oxygen to form water molecules (electron donating path) and formation of the OH^- (electron accepting path). The first process takes place at lower temperatures, while the formation of OH^- - radicals is observed at higher temperatures.

Finally, to estimate the role of the bottlenecked segments in sensing performance of the SMNW, the comparative series of measurements were carried out (in the same run) on a straight SnO_2 NW of the similar length and a diameter of ~100 nm. It was established that the sensitivity S of straight NS measured even at a little bit higher hydrogen pressure $P_{H2}=4x10^{-4}$ amounted to only 40%; that is, it is lower than in the case of SMNW. Since the straight NW diameter is ~3 times smaller than the average diameter (D~290 nm) of the structurally modified (containing large and narrow segments) NS, we could expect that sensitivity of the straight NW will be higher. However, we observe the opposite situation; in our opinion, it is attributed to the role played by the narrowed (~ 40-80 nm) segments in the NW conductance. In some degree, it is similar to the intergrain effects in nano/microcrystalline films or ceramic powder nanomaterials (Fig. 8a). However, in our case, we have monocrystalline NS, in which larger-diameter segments are alternating with narrow "necks" (Fig. 8b). These narrow segments, due to their smaller diameters and, as a result, smaller diameters of the conduction channel X_2, are more sensitive to gas atmosphere changing, because at the same depth of modulation of the depletion region, the conduction channel width in the narrow segment X_2 will be smaller by a few times or even by an order than the same parameter X_1 in the large-diameter segment. At the interaction with ambient gas, this narrowed part of SMNW will be most sensitive to the presence of different gases on its surface due to the faster depletion of the NW.

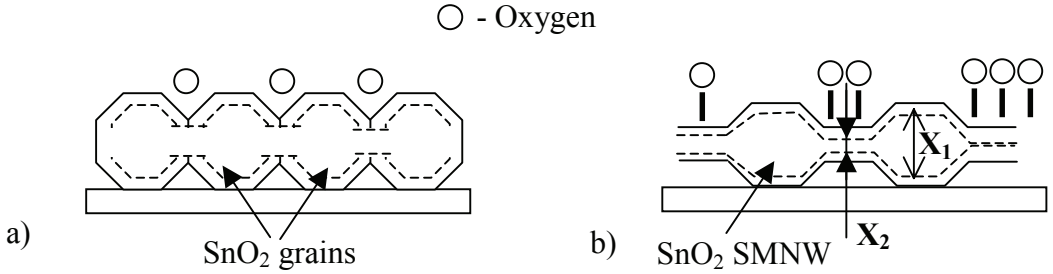

Fig. 8. Schematic presentation of interaction of the polycrystalline SnO_2 thin film and single crystal SnO_2 SMNW with oxygen. The dashed line shows the level of charge carrier depletion.

The main difference between the two cases presented in Fig. 8 is that narrowed segments are being the part of the same NW; that is, the NW single-crystal morphology is preserved. The later makes it possible, in comparison with granular structures, to minimize or exclude such undesirable effects as aging, thermal, mechanical, and chemical instabilities in local intergrain interfaces.

Conclusions

It is shown that structurally modified single-crystal NSs can be successfully used in gaseous sensorics in the ppm and sub-ppm range.

The developed approach gives the possibility for structural modification of NWs, controlling their electronic and, as a result, gas sensing properties. Varying the carrier gas flux during NW formation, we not only can change the direction of NW growth and provide the changing of NW geometrical size but also we can technologically get the "necks" within the same single crystal. The basic advantage of such monocrystalline quasi-1D nanosensors over the traditional sensors on the basis of nanostructured (nanogranular) thin film consists in the absence of the unstable intergrain contacts. In fact, we obtain an additional tool for NSs engineering, which renders possible to design a nanodevice for specific applications.

Acknowledgements

The author would like to thank Dr. A. Kolmakov for the possibility to carry out the research in the Laboratory of the Surface Phenomena & Imaging of Nanostructures (Southern Illinois University –Carbondale (SIUC), USA). The performed research was supported via SIUC Seed Grant and in part through the Materials Technology Center (SIUC) Grant.

References

[1] Y. Cui, Q.Q. Wei, H.K. Park, and C.M. Lieber, Science, 293, 1289, (2001).
[2] M. Law, H. Kind, B. Messer, F. Kim, and P.D. Yang, Angewandte Chemie-International Edition, 41, 2405, (2002).
[3] E. Comini, G. Faglia, G. Sberveglieri, Z.W. Pan, and Z.L. Wang, Applied Physics Letters, 81, 1869, (2002).
[4] M.S. Arnold, P. Avouris, Z.W. Pan, and Z.L. Wang, Journal of Physical Chemistry B, 107, 659, (2003).
[5] C. Li, D.H. Zhang, X.L. Liu, S. Han, T. Tang, J. Han, and C.W. Zhou, Applied Physics Letters, 82, 1613, (2003).
[6] A. Kolmakov, Y.X. Zhang, G.S. Cheng, and M. Moskovits, Advanced Materials, 15, 997, (2003).
[7] Y.L. Wang, X.C. Jiang, and Y.N. Xia, Journal of the American Chemical Society, 125, 16176, (2003).
[8] A. Kolmakov and M. Moskovits, Annual Review of Materials Research, 34, 151, (2004).
[9] D.H. Zhang, Z.Q. Liu, C. Li, T. Tang, X.L. Liu, S. Han, B. Lei, and C.W. Zhou, Nano Letters, 4, 1919, (2004).
[10] Z.Y. Fan, D.W. Wang, P.C. Chang, W.Y. Tseng, and J.G. Lu, Applied Physics Letters, 85, 5923, (2004).
[11] B.J. Murray, E.C. Walter, and R.M. Penner, Nano Letters, 4, 665, (2004).
[12] R.E. Cavicchi, S. Semancik, F. DiMeo, and C.J. Taylor, Journal of Electroceramics, 9, 155, (2003).
[13] M.E. Franke, T.J. Koplin, and U. Simon, Small, 2, 36, (2006).
[14] G. Eranna, B.C. Joshi, D.P. Runthala, and R.P. Gupta, Critical Reviews in Solid State and Materials Sciences, 29, 111, (2004).
[15] N. Barsan, M. Schweizer-Berberich, and W. Gopel, Fresenius Journal of Analytical Chemistry, 365, 287, (1999).
[16] Z.R. Dai, Z.W. Pan, and Z.L. Wang, Advanced Functional Materials, 13, 9, (2003).
[17] A. Kolmakov, D.O. Klenov, Y. Lilach, S. Stemmer, and M. Moskovits, Nano Letters, 5, 667, (2005).
[18] S. Dmitriev, Y. Lilach, B. Button, M. Moskovits, A. Kolmakov, Nanotechnology, 18, 055707, (2007).
[19] S. Samson and C.G. Fonstad, J. Appl. Phys., 44, 4618, (1973).